# Synthesis, Characterization and Photoconductivity studies on nanocrystalline $TiO_2$ films doped with gold nanoparticles

G. Valverde-Aguilar [1], J. A. García-Macedo [1*], P. Galván-Ramírez[1], V. Rentería-Tapia [1]

1. Departamento de Estado Sólido. Instituto de Física, Universidad Nacional Autónoma de México. México D. F. C. P. 04510

*** Contact author:**
Dr. Jorge Garcia Macedo
Instituto de Física, UNAM
Circuito de la Inv. Científica s/n
C. P. 04510. Del. Coyoacán
México, D.F.
México.
Tel. (5255) 5622–51–03
Fax (5255) 5616–15–35
E–mail: gamaj@fisica.unam.mx

## ABSTRACT

Nanocrystalline $TiO_2$ films doped with gold nanoparticles were synthesized by the sol–gel process at room temperature. The $TiO_2$ films were synthesized by using tetrabutyl orthotitanate as the inorganic precursor. The films were spin-coated on glass wafers. The samples were annealed at 100°C for 30 minutes and sintered at 520°C for 1 hour to generated anatase and rutile phases. The films were characterized using UV-Vis absorption spectroscopy, X-ray diffraction, Fourier transform infrared spectroscopy and scanning electron microscopy. An absorption peak located at around 651 nm is due to the surface plasmon resonance of the gold nanoparticles. Optical absorption spectrum was fitted by Gans model by using a high refractive index ($n_{local}$ = 2.6). This high index is related to the high content of anatase nanoparticles embedded in the film. Photoconductivity studies were performed on nanocrystalline (anatase phase) films. The experimental data were fitted with straight lines at darkness and under illumination at 515 nm and 645 nm. This indicates an ohmic behavior. Transport parameters were calculated. Results are discussed.

KEYWORDS: Titania, gold nanoparticles, sol-gel, thin film, photoconductivity, spin-coating, Gans theory, refractive index

## 1. INTRODUCTION

Titanium dioxide ($TiO_2$) is a non-toxic material. $TiO_2$ thin films exhibit high stability in aqueous solutions and no photocorrosion under band gap illumination and special surface properties. $TiO_2$ thin films are already widely used in the study of the photocatalysis and photoelectrocatalysis of organic pollutants [1, 2]. Photoelectrocatalytic system has received a great deal of attention due to drastically enhanced quantum efficiency [3]. By applying small bias, recombination of generated electron–hole pairs is retarded.

$TiO_2$ is the subject of intensive research, especially with regard to its end uses in solar cells, chemical sensors, photoelectrochemical cells, photocatalysis and electronic devices [4, 5]. Due to its wide-ranging chemical and physical properties (electrical conductivity, photosensitivity, aqueous environments) $TiO_2$ has a large variety

Nanophotonic Materials VI, edited by Stefano Cabrini, Taleb Mokari, Proc. of SPIE Vol. 7393, 73930X · © 2009 SPIE · CCC code: 0277-786X/09/$18 · doi: 10.1117/12.826730

of potential applications. As a wide band gap semiconductor, $TiO_2$ shows a diverse heterogeneity of crystalline phases, whereby it is possible to find it in anatase, rutile or brookite form [6].

$TiO_2$ are almost impossible to measure in great detail in powder form, due to the difficulty in manipulating grain sizes in the range of 1–50 nm [7]. Furthermore, measurements carried out on powder represent only an average value for many grains oriented in all possible directions. This difficulty in working with powder samples, together with the ongoing search for new applications, has compelled many researchers to work with $TiO_2$ thin films instead.

In the present work, we described the synthesis, characterization and photoconductivity behaviour of nanocrystalline $TiO_2$ films doped with gold nanoparticles (NP's). The films were produced by the sol–gel process at room temperature by using the spin-coating method and deposited on glass wafers. The samples were sintered at 520°C for 1 hour. The obtained films were characterized by X-ray diffraction (XRD), optical absorption (OA), Fourier transform infrared spectroscopy (FTIR) and scanning electron microscopy (SEM) studies. Photoconductivity studies were performed on nanocrystalline films (anatase and rutile phases). Transport parameters were calculated.

## 2. EXPERIMENTAL

Glass substrates were cleaned in boiling acidic solution of sulphuric acid-$H_2O_2$ (4:1) under vigorous stirring for 30 minutes. They were then placed in deionized water and boiled for 30 minutes, rinsed three times with deionized water and stored in deionized water at room temperature.

*Preparation of $TiO_2$ solution.* All reagents were Aldrich grade. The precursor solutions for $TiO_2$ films were prepared by the following method. Tetrabutyl orthotitanate and diethanolamine ($NH(C_2H_4OH)_2$) which prevent the precipitation of oxides and stabilize the solutions were dissolved in ethanol. After stirring vigorously for 2h at room temperature, a mixed solution of deionized water and ethanol was added dropwise slowly to the above solution with a pipette under stirring. Finally, Tetraethyleneglycol (TEG) was added to the above solution. This solution is stirred vigorously to obtain an uniform sol. The resultant alkoxide solution was kept standing at room temperature to perform hydrolysis reaction for 2h, resulting in the $TiO_2$ sol.

*Preparation of Au stock solution*. 0.03 M of Hydrogen Tetrachloroaurate(III) hydrate ($HAuCl_4 \cdot aq$) was dissolved in a mixture of deionized water and ethanol. It was stirred for 5 minutes.

The Au stock solution was added to 20 ml of $TiO_2$ solution. This final solution was stirred for 17 hours at room temperature to obtain a purple colour. The final chemical composition of this solution was $Ti(OC_4H_9)_4$ : $NH(C_2H_4OH)_2$ : $C_2H_5OH$ : DI $H_2O$ : TEG: nitric acid: $HauCl_4$ = 1:1: 14.1:1:1.028:0.136:0.024. The $TiO_2$ with gold NP's solution has a pH = 6.0. The $TiO_2$ films were prepared by the spin-coating technique. The precursor solution was placed on the glass wafers (2.5 x 2.5 $cm^2$) using a dropper and spun at a rate of 3000 rpm for 20 s (Figure 1).

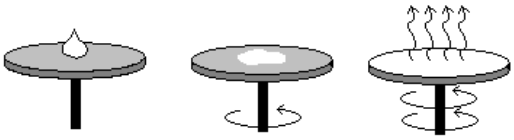

Figura 1. Spin-coating technique.

After coating, the film was dried at 100 °C for 30 min in a muffle oven and sintered at 520 °C for 1 h in a muffle oven in order to remove organic components. The procedure was repeated two times to achieve the film thickness with two layers. The films show a light blue colour.

UV-vis absorption spectra were obtained on a Thermo Spectronic Genesys 2 spectrophotometer with an accuracy of ±1 nm over the wavelength range of 300-900 nm. The structure of the final films was characterized by XRD patterns. These patterns were recorded on a Bruker AXS D8 Advance diffractometer using Ni-filtered CuK$\alpha$ radiation. A step-scanning mode with a step of 0.02° in the range from 1.5 to 60° in $2\theta$ and an integration time of 2 s was used. FTIR spectra were obtained from a KBr pellet using a Bruker Tensor 27 FT-IR spectrometer. Pellets were made from a finely ground mixture of the sample and KBr at a ratio of KBr:sample = 1:0.019. The thickness of the films was measured using a SEM microscopy Model STEREOSCAN at 20 kV.

For photoconductivity studies [9] silver electrodes were painted on the sample. It was maintained in a $10^{-5}$ Torr vacuum cryostat at room temperature in order to avoid humidity. For photocurrent measurements, the films were illuminated with light from an Oriel Xe lamp passed through a 0.25m Spex monochromator. Currents were measured with a 642 Keithley electrometer connected in series with the voltage power supply. The applied electrostatic field E was parallel to the film. Light intensity was measured at the sample position with a Spectra Physics 404 power meter (Figure 2).

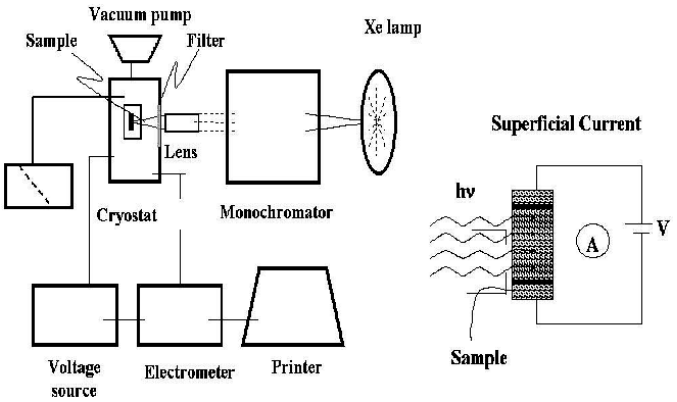


Figure 2. Schematic diagram of the photoconductivity technique. Superficial current was produced on the thin film when an electric field was applied to it.

## 3. RESULTS AND DISCUSSION

**3.1 X-ray diffraction patterns.** The X-ray diffraction pattern of the nanocrystalline $TiO_2$ film with gold NP's is presented in Figure 3. The films sintered at 520 °C for 1 hour exhibit very good crystallization that corresponds to anatase and rutile phases. The anatase phase was identified by the diffraction peaks located at 2θ =25.33, 38.17, 48.01, 53.96 and 55.20 which can be indexed as (101), (112), (200), (105) and (211) respectively. The rutile phase was identified by the diffraction peaks located at 2θ = 27.47, 36.10, 40.03, 44.35, 64.62 and 77.65 which can be indexed as (110), (101), (200), (210), (310) and (202) respectively. The position of the diffraction peaks in the film is in good agreement with those given in ASTM data card (#21-1272) for anatase and ASTM data card (#21-1276) for rutile.

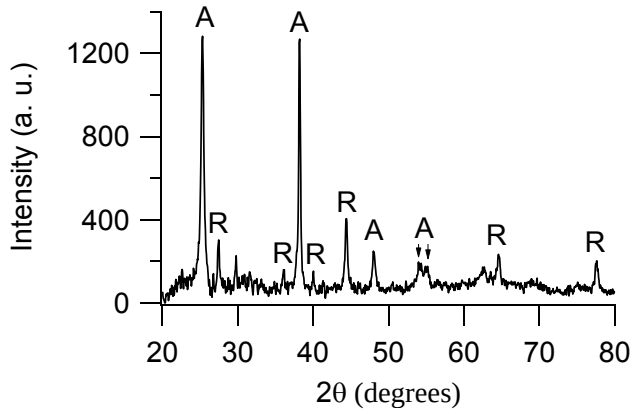


Figure 3. X-ray diffraction pattern at high angle of the nanocrystalline $TiO_2$ film with gold NP's sintered at 520 °C for 1 hour.

The average nanocrystalline size (D) was calculated from Scherrer´s formula [10] by using the diffraction peak (101) for anatase phase and the peak (110) for rutile phase:

$$D = \frac{0.9\lambda}{B\cos\theta} \qquad (1)$$

with $\lambda$=1.54056x10$^{-10}$ m. Table 1 contains the results.

The weight fractions of rutile ($x_r$) and anatase ($x_a$) present in the film samples can be calculated by the following equations respectively [11]:

$$x_r = \frac{I_r}{0.884I_a + I_r}, \qquad x_a = \frac{0.884I_a}{0.884I_a + I_r} \qquad (2)$$

where $I_r$ and $I_a$ are the integrated intensities of rutile (110) and anatase (101) peaks. These calculations are shown in Table 1.

Table 1.Summary of nanoscopic characteristics of nanocrystalline $TiO_2$ film with gold NP's.

| Phase | B | Radian | D (nm) | Crystal phase (wt%) |
|---|---|---|---|---|
| Anatase (101) | 0.44° | 0.00768 | 18.5 | 83.5 |
| Rutile (110) | 0.3112 ° | 0.00543 | 26.3 | 16.5 |

**3.2 Optical absorption.** Figure 4 shows the optical absorption spectra of the nanocrystalline $TiO_2$ thin films with gold NP's taken at room temperature in the range of 300-900 nm. The spectrum of the film calcined at 450 °C for 15 min shows an absorption band A located at 402 (3.08 eV) corresponding to the $TiO_2$ and a second band B located 651 nm (1.93 eV) corresponding to the surface plasmon resonance (SPR) of the gold NP's.

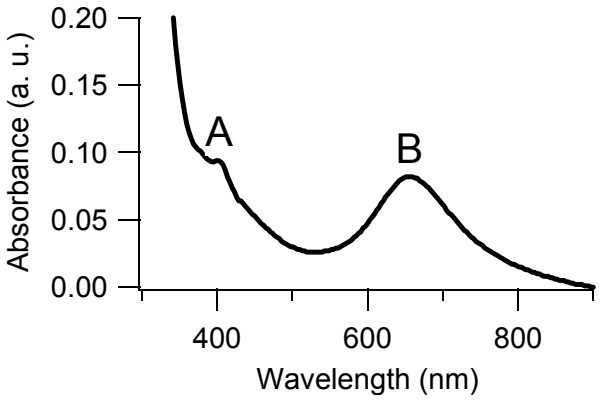


Figure 4. Absorption spectrum of the nanocrystalline $TiO_2$ film with gold NP's.

Literature [8, 9] reports an absorption peak for surface plasmon resonance (SPR) of gold nanoparticles around 500-550 nm. In our samples, a red-shift of absorption peak from 550 to 651 nm was observed. This fact is originated to the increase in the diameter of Au nanoparticles and an increment of the refractive index of $TiO_2$ matrix with increasing the heat-treatment temperature [12, 13]. It is known that the refractive index of $TiO_2$ films is related to the crystal phase (anatase or rutile), the crystalline size and the densities of the films [14].

The optical absorption spectrum (Fig. 4) was fitted very well using Gans theory [15] with a local refractive index $n_{local}$ = 2.6 (Figure 5). This index has a value close to the refractive index reported for the anatase phase ($n_{anatase}$ = 2.54) [16]. This is consistent with the fact we have anatase phase in a proportion of 83.5 wt% according to the X-ray diffraction pattern (Fig. 3), while the rutile phase ($n_{rutile}$ = 2.75) [16] has a proportion of 16.5 wt%.

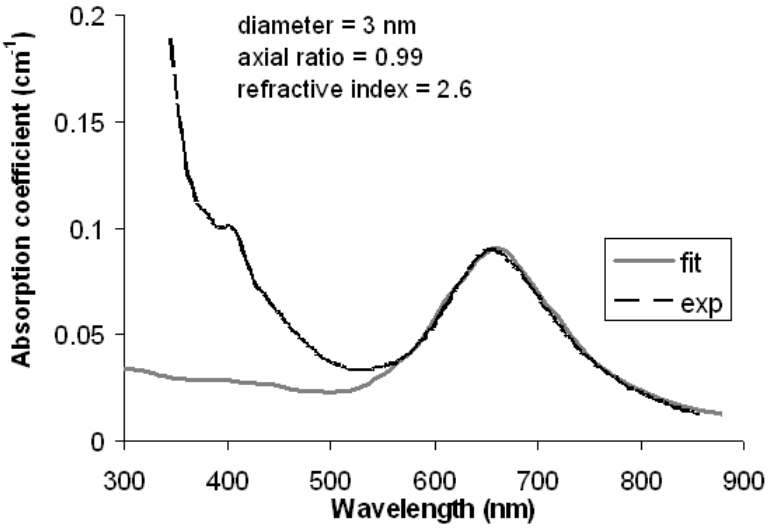


Figure 5. Experimental optical absorption spectrum (black dotted line) of the nanocrystalline $TiO_2$ film with gold NP's. The calculated optical absorption spectrum (grey solid line) obtained by Gans theory.

The optical band-gap, Eg, was determined from the absorption spectrum, (Fig. 4) using equation [17]:

$$(\alpha h\nu)^2 = C(h\nu - E_g) \qquad (4)$$

where $\alpha$ is the absorption coefficient, $h\nu$ is the photon energy, $E_g$ is the band gap energy and C depends on the electron-hole mobility.

The $(\alpha h\nu)^2$ vs. $h\nu$ plot is displayed in Figure 6. The value of $E_g$ was determined plotting a tangent line (black solid line) to the curve. The value of 3.57 eV (it is marked with a cross) is slightly bigger than the optical band-gap reported for similar monocrystalline $TiO_2$ films [8].

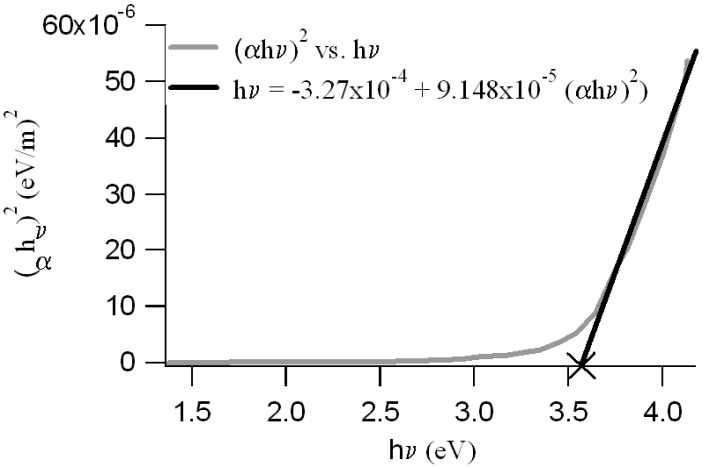


Figure 6. Evolution of the $(\alpha h\nu)^2$ vs. $h\nu$ curve of nanocrystalline $TiO_2$ film with gold NP's (grey solid line). The value of $E_g$ of 3.57 eV is marked with a cross.

**3.3 SEM measurements.** The thickness of the films was measured by SEM technique. Figure 7 shows the SEM image for nanocrystalline $TiO_2$ film with gold NP's, the thickness is $1.7 \pm 0.3$ μm.

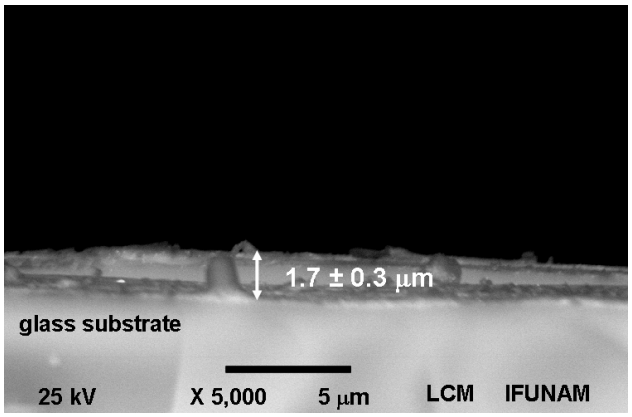


Figure 7. Cross-sectional SEM image of nanocrystalline $TiO_2$ film with gold NP's sintered at 520 °C for 1 hour.

.

**3.4 FTIR analysis.** Figure 8 shows FTIR spectrum of nanocrystalline $TiO_2$ film prepared as KBr pellet. The band seen at 438 $cm^{-1}$ and 490 $cm^{-1}$ correspond to the $\nu_{Ti\text{-}O\text{-}Ti}$ stretching vibration in the anatase phase [18, 19]. The strong bands centered at 1263 and 1113 $cm^{-1}$ originate in the C-O-C bonds of TEG [19, 20]. The peak located at 2926 $cm^{-1}$ is due to asymmetric C–H bond in existence of DEA [21]. Table 2 contains the bands of nanocrystalline $TiO_2$ sample and their description.

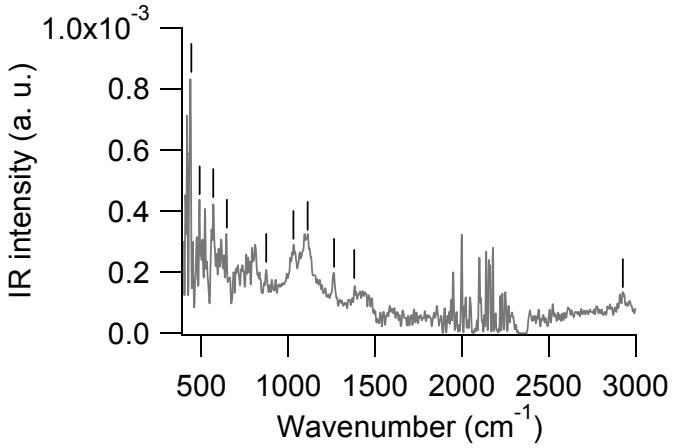


Figure 8. FTIR spectrum of nanocrystalline $TiO_2$ film with gold NP's annealed at 520 °C for 1 hour. The sample was prepared as KBr pellet.

Table 2. IR frequencies [in cm-1] of the nanocrystalline TiO2 film with gold NPôs.

| Nanocrystalline | | |
|---|---|---|
| $\bar{\nu}_{exp}$ (cm$^{-1}$) | description | Ref |
| 438 | $\nu_{Ti\text{-}O\text{-}Ti}$ (anatase) | 20, 21 |
| 490 | $\nu_{Ti\text{-}O\text{-}Ti}$ (anatase) | 20 |
| 569 | $\nu_{Ti\text{-}O}$ | 20 |
| 644 | $\nu_{Ti\text{-}O}$ | 20 |
| 876 | TEG | Aldrich |
| 1032 | - | - |
| 1113 | C–O–C bond of TEG | 21 |
| 1263 | C–O–C bond of TEG | 21, 22 |
| 1382 | $NO_3$ | 20 |
| 2926 | asymmetric C-H bond (DEA) | 23 |

**3.5 Photoconductivity studies.** Usually [9] Ohm's law under light illumination is given by

$$\vec{J} = \vec{J}_{ph} + (\sigma_d + \sigma_{ph})\vec{E}, \tag{5}$$

where $\vec{J}_{ph}$ is the photovoltaic current density, and $\sigma_{ph}$ is the photoconductivity. When the current densities are assumed to be parallel to the electric field $\vec{E}$ Eq. (5) becomes into the next one:

$$J = \frac{q\phi l_0 \alpha I}{h\nu} + \left(\sigma_d + \frac{q\phi\mu\tau\alpha I}{h\nu}\right)E, \tag{6}$$

with $\phi$ as the quantum yield of charge carrier photogeneration, $l_0$ as the charge carrier mean free path, $\alpha$ as the sample absorption coefficient, $I$ as the light intensity at the frequency $\nu$ of illumination, $h$ as the Planck´s constant, and $\tau$ as the charge carriers mean lifetime. The first term is the photovoltaic transport effect, the second one is the dark conductivity $\sigma_d = en_0\mu$, and the third one is the photoconductivity itself.

Eq (6) can be written as:

$$J = A_1 E + J_0 \tag{7}$$

From the absorption spectrum of nanocrystalline film (Fig. 4), the illumination wavelength for photoconductivity studies were chosen: 645 nm that corresponds to the maximum absorption band and 515 nm were there is no absorption. Photoconductivity results of nanocrystalline $TiO_2$ films with gold NP's are shown in Figure 9. Current density as function of electric applied field on the film was plotted. The experimental data were fitted by least-squares with straight lines at darkness and under illumination (515 nm, 645 nm). This indicates an ohmic behaviour. The linear fits are shown in Table 3.

For these samples, when the illumination wavelength decreases the slope $A_1$ increases. On the other hand, when the illumination wavelength decreases, $J_0$ decreases.

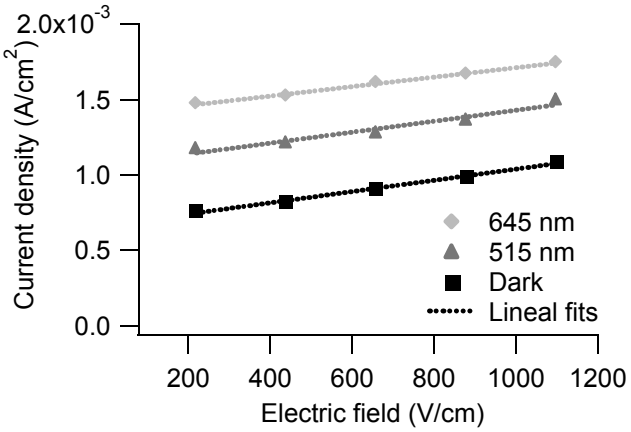


Figure 9. Experimental data of current density vs. electric field spectra from nanocrystalline $TiO_2$ film with gold NP's. Linear fits correspond to the dotted lines.

Table 3. Linear fittings of nanocrystalline $TiO_2$ films.

| λ (nm) | $A_1$ | $J_0$ |
|---|---|---|
| 645 | $3.14 \times 10^{-7}$ | $1.40 \times 10^{-3}$ |
| 515 | $3.64 \times 10^{-7}$ | $1.07 \times 10^{-3}$ |
| Darkness | $3.73 \times 10^{-7}$ | $6.66 \times 10^{-4}$ |

With the equation (6), by measuring I, the dark conductivity and the conductivity under illumination at 645 and 355 nm, and fitting the experimental data by the least squares method, as it is shown in Fig. 9, the photoconductive ($\phi\mu\tau$) and photovoltaic ($\phi l_0$) parameters were obtained (Table 4). The photovoltaic parameter ($\phi l_0$) increases when the wavelength decreases. This indicates a strong photovoltaic behaviour. The photoconductive parameter ($\phi\mu\tau$) decreases when the wavelength is changed to maximum absorption. This indicates a strong photoconductive effect.

Table 4. Photovoltaic and photoconductive parameters of nanocrystalline $TiO_2$ films with gold NP's.

| Parameter | 645 nm | 515 nm |
|---|---|---|
| $\phi l_0$ (cm) | $9.71 \times 10^{-4}$ | $1.41 \times 10^{-3}$ |
| $\phi\mu\tau$ ($cm^2/V$) | $7.87 \times 10^{-8}$ | $3.42 \times 10^{-8}$ |

## 4. CONCLUSIONS

High optical quality nanocrystalline $TiO_2$ films with gold NP's were obtained by sol-gel process. XRD measurements reveal the presence of the anatase and rutile phases, which were produced after sintering treatment of 520 °C for 1h. The anatase phase has a bigger proportion (83.5 wt%) than the rutile phase (16.5 wt%).

The optical absorption spectrum was fitted very good using Gans theory by using a local refractive index $n_{local} = 2.6$. This index is related to the major crystal phase, anatase.

Photoconductivity studies on these films were done. The experimental data was fitted by straight lines corresponding to an ohmic behaviour. The $\phi l_0$ and $\phi\mu\tau$ parameters indicate a strong photovoltaic and photoconductive behaviour.

## ACKNOWLEDGMENTS

The authors acknowledge the financial supports of CONACYT 79781, CONACyT 89584, NSF-CONACYT, PUNTA, ICYTDF and PAPIIT 116506-3. GVA is grateful for ICyTDF postdoctoral fellowship. The authors are thankful to M. in Sci. Manuel Aguilar-Franco (XRD), Luis Rendón (HRTEM), Roberto Hernández-Reyes (SEM) and Diego Quiterio (preparation of the samples for SEM studies) for technical assistance.

## REFERENCES

[1] Suarez, R., Nair, P. K. Kamat, P. V., "Photoelectrochemical Behavior of $Bi_2S_3$ Nanoclusters and Nanostructured –Thin Films", Langmuir 14(12), 3236-3241 (1998).
[2] Shaogui, Y., Xie, Q., Xinyong, L., Yazi, L., Shuo, C., Guohua, C., "Preparation, characterization and photoelectrocatalytic properties of nanocrystalline $Fe_2O_3/TiO_2$, $ZnO/TiO_2$, and $Fe_2O_3/ZnO/TiO_2$ composite film electrodes towards pentachlorophenol degradation", Phys. Chem. Chem. Phys. 6(3), 659-664 (2004).
[3] Kim, D. W., Lee, S., Jung, H. S., Kim, J. Y., Shin, H., Hong, K. S., "Effects of heterojunction on photoelectrocatalytic properties of $ZnO$-$TiO_2$ films", International Journal of Hydrogen Energy 32(15), 3137–3140 (2007).
[4] Graziani Garcia, C., Murakami Iha, N-Y., Argazzi, R., Bignozzi, C.-A., "4-Phenylpyridine as ancillary ligand in ruthenium (II) polypyridyl complexes for sensitization of n-type $TiO_2$ electrodes", J. Photochem. Photobiol. A: Chem. 115(3), 239-242 (1998).
[5] Dueñas, S., Castán, H., García, H., San Andrés, E., Toledano-Luque, M., Mártil, I., González-Díaz, G., Kukli, K., Uustare, T., Aarik, J., "A comparative study of the electrical properties of $TiO_2$ films grown by high-pressure reactive sputtering and atomic layer deposition", Semicond. Sci. Technol. 20(10), 1044-1051 (2005).
[6] Hu, L., Yoko, T., Kosuka, H., Sakka, S., "Effects of solvent on properties of sol-gel derived $TiO_2$ coating films", Thin Solid Films 219(1-2), 18-23 (1992).
[7] Gerischer, H.,. Heller, A., "Photocatalytic Oxidation of Organic Molecules at $TiO_2$ Particles by Sunlight in Aerated Water", J. Electrochem. Soc. 139(1), 113-118 (1992).
[8] Yu, J., Yue, L., Liu, S., Huang, B., Zhang, X., "Hydrothermal preparation and photocatalytic activity of mesoporous Au–$TiO_2$ nanocomposite microspheres", J. Colloid and Interf. Sci. 334(1), 58–64 (2009).
[9] García M., J., Mondragón, A., Hernández, J. M., Maldonado R., J. L., "Photocurrent determination of charge transport parameters in $KNbO_3$:$Fe^{3+}$", Opt. Mat., 3(1), 61-64 (1994).
[10] Wilson, G. J., Matijasevich, A. S., Mitchell, D. R. G., Schulz, J. C., Will, G. D., "Modification of $TiO_2$ for Enhanced Surface Properties: Finite Ostwald Ripening by a Microwave Hydrothermal Process", Langmuir 22(5), 2016-2027 (2006).
[11] Chen, W., Geng, Y., Sun, X.-D., Cai, Q., Li, H.-D., Weng, D., "Achievement of thick mesoporous $TiO_2$ crystalline films by one-step dip-coating approach", Microporous and Mesoporous Materials 111(1-3), 219–227 (2008).
[12] Ito, A., Masumoto, H., Goto, T., "Optical Properties of Au Nanoparticle Dispersed $TiO_2$ Films Prepared by Laser Ablation", Materials Transactions 44(8), 1599-1603 (2003).
[13] Liz-Marzán, L. M., Giersig, M., Mulvaney, P., "Synthesis of Nanosized Gold-Silica Core-Shell Particles", Langmuir 12(18), 4329-4335 (1996).
[14] Brinker, C. J., Frye, G. C., Hurd A. J., Ashley, C. S. "Fundamentals of sol-gel dip coating", Thin Solid Films 201(1), 97-108 (1991).
[15] Rentería, V. M., García–Macedo, J., "Influence of the local dielectric constant on modeling the optical absorption of silver nanoparticles in silica gels", Colloids and Surfaces A: Physicochemical and Engineering Aspects, 278(1-3), 1-9 (2006).
[16] Wang, Z., Helmersson, U., Käll, P.-O., "Optical properties of anatase $TiO_2$ thin films prepared by aqueous sol–gel process at low temperature", Thin Solid Films 405, 50–54 (2002).
[17] Tauc, J., Grigorovichi, R., Vancu, A., "Optical properties and electronic structure of amorphous germanium", Phys. Status Solidi. 15(2), 627–633 (1966).
[18] Music, S., Gotic, M., Ivanda, M., Popovic, S., Turkovic, A., Trojko, R., Sekulic, A., Furic, K., "Chemical and micro structural properties of $TiO_2$ synthesized by sol-gel procedure", Mat. Sci. and Eng. B 47(1), 33-40 (1997).
[19] Djaoued, Y., Badilescu, S., Ashrit, P. V., Bersani, D., Lottici, P. P., "Study of Anatase to Rutile Phase Transition in Nanocrystalline Titania Films", J. Sol-Gel Sci. & Techn. 24(3), 255–264 (2002).

[20] Djaoued, Y., Badilescu, S., Ashrit, P. V., "Low Temperature Sol-Gel Preparation of Nanocrystalline $TiO_2$ Thin Films", J. Sol-Gel Sci. & Techn. 24(3), 247–254 (2002).
[21] Cheng, X. L., Zhao, H., Huo, L. H., Gao, S., Zhao, J. G., "ZnO nanoparticulate thin film: preparation, characterization and gas-sensing property", Sensors and Act. B 102(2), 248-252 (2004).